

## Supplementary Information

### Substituent-dependent reactivity of triarylantimony(III) toward I<sub>2</sub>: isolation of [Ar<sub>3</sub>SbI]<sup>+</sup> salt

Vladimir V. Sharutin, Olga K. Sharutina, Alexander S. Novikov and Sergey A. Adonin

#### Synthetic procedures

All reagents were obtained from commercial sources and used as purchased. Tris(p-tolyl) (a), tris(m-tolyl) (b), tris(4-fluorophenyl) (c) and tris(2-methoxy-5-bromophenyl)antimony (d) precursors were obtained following the procedures reported earlier:

- a) Kocheshkov K.A. et al. Methods of organoelement chemistry. Antimony and Bismuth. Moscow Nauka, 1976, 483 p. (in Russian)
- b) Kocheshkov K.A. et al. Methods of organoelement chemistry. Antimony and Bismuth. Moscow Nauka, 1976, 483 p. (in Russian)
- c) De Ketelaere R.F., Delbeke F.T., Van der Kelen G.P. // J. Organometal. Chem. 1971. V. 30. P. 365.
- d) Sharutin V.V., Senchurin V.S., Sharutina O.K., Chagarova O.V. // Russ. J. Inorg. Chem. 2011. Vol. 56. N 10. P. 1561.

All solvents were purified according to the standard procedures. All experiments were carried out in N<sub>2</sub> atmosphere.

#### Syntheses of 1-3

0.25 mmol of Ar<sub>3</sub>Sb were dissolved in 10 ml of benzene, followed by addition of 0.25 mmol of I<sub>2</sub>. The mixtures were stirred for 1 h at room temperature. After that, 1 ml of n-octane was added and the solvent was evaporated to 2 ml, resulting in formation of colorless crystals of **1**, **2** or **3**. Yields: 56% (**1**), 92% (**2**), 86% (**3**), m.p. 182, 131 and 163°C, respectively.

**Table S1.** Element analysis data for **1-3**

Compound	C, H (calcd)	C, H (found)
<b>1</b>	38.83; 3.24	38.68; 3.28
<b>2</b>	38.83; 3.24	38.75; 3.32
<b>3</b>	32.68; 1.81	32.57; 1.89

**Table S2.** NMR characteristics for **1-3** (NMR spectra were measured on Bruker Advance 500 NMR spectrometer)

Compound	<sup>13</sup> C NMR	<sup>1</sup> H NMR
<b>1</b>	21.3 (methyl), 129.0, 135.8, 136.4, 138.4 (aryl)	2.17 (3H), 7.44 (m-H), 7.95 (o-H)

<b>2</b>	20.4 (methyl), 129.4, 129.6, 130.0, 132.4, 133.2, 139.7 (aryl)	2.27 (3H), 7.38, 7.44, 7.51, 7.89
<b>3</b>	116.8, 135.0, 136.1, 165.2	7.20, 7.36

### Synthesis of 4

In initial experiment, 0.25 mmol of  $(2\text{-MeO-5-BrPh})_3\text{Sb}$  reacted with equimolar amount of  $\text{I}_2$  as described for **1-3**. In this case, we isolated **4** and initial  $(2\text{-MeO-5-BrPh})_3\text{Sb}$  in approx. 1:1 ratio. Therefore, for preparation of pure **4**, 0.5 mmol of  $\text{I}_2$  were used to give only **4** (yield 69%). T. decomp. 110°C, for  $\text{C}_{21}\text{H}_{18}\text{Br}_3\text{I}_4\text{O}_3\text{Sb}$  calcd, %: C, 21.29; H, 1.53; found, %: C, 21.17; H, 1.59.

### X-ray Diffractometry.

**XRD for 1-4** was performed on D8 QUEST Bruker diffractometer ( $\text{MoK}_\alpha$ ,  $\lambda = 0.71073 \text{ \AA}$ , graphite monochromator) at 293 K. Integration, absorption correction, and determination of unit cell parameters were performed using SMART and SAINT-Plus software (Bruker (1998). SMART and SAINT-Plus. Versions 5.0. Data Collection and Processing Software for the SMART System. Bruker AXS Inc., Madison, Wisconsin, USA). The structures were solved by dual space algorithm (SHELXT) and refined by the full-matrix least squares technique (SHELXL) in the anisotropic approximation (except hydrogen atoms) as inversion twin. Positions of hydrogen atoms of organic ligands were calculated geometrically and refined in the riding model. Details are summarized in Table S1. CCDC 1989078 (**1**), 1987109 (**2**), 1989015 (**3**) and 1980084 (**5**) contain the supplementary crystallographic data for this paper.

**Table S3.** Details of XRD experiments for **1-4**

Parameter	<b>1</b>	<b>2</b>	<b>3</b>	<b>4</b>
Empirical formula	$C_{21}H_{21}Br_{0.60}I_{1.40}Sb$	$C_{21}H_{21}I_2Sb$	$C_{18}H_{12}F_3I_2Sb$	$C_{21}H_{18}Br_3I_4O_3Sb$
$M$ , g/mol	620.73	648.93	660.83	1187.43
Crystal system, space group	Cubic, $P4_332$	Monoclinic, $P2_1/c$	Triclinic, $P-1$	Triclinic, $P-1$
a,b,c, Å	13.0818 (15)	15.213 (3), 15.643 (3), 9.2291 (18)	8.6690 (17), 9.4881 (19), 13.136 (3)	9.4322 (19), 12.154 (2), 13.144 (3)
$\alpha, \beta, \gamma$ , °	90	90, 93.34 (3), 90	85.17 (3), 84.75 (3), 73.62 (3)	87.26 (3), 80.96 (3), 82.24 (3)
$V$ , Å <sup>3</sup>	2238.7 (8)	2192.7 (8)	1030.3 (4)	1474.0 (5)
Z	4	4	2	2
$F(000)$	1173	1216	608	1072
$\theta$ range (°) for cell measurement	3.1–32.5	2.8–34.5	3.1–27.9	3.0–25.9
$\mu$ (mm <sup>-1</sup> )	4.23	4.07	4.36	9.21
Crystal size (mm)	0.26 × 0.17 × 0.09	0.49 × 0.34 × 0.21	0.28 × 0.18 × 0.12	0.29 × 0.16 × 0.11
$T_{\min}, T_{\max}$	0.579, 0.746	0.410, 0.747	0.532, 0.746	0.175, 0.431
No. of measured, independent and observed [ $I > 2\sigma(I)$ ] reflections	26013, 720, 685	56515, 4162, 3626	27698, 3907, 3003	22024, 5461, 4191
$R_{\text{int}}$	0.029	0.036	0.032	0.039
$\theta$ values (°)	$\theta_{\max} = 25.7$ , $\theta_{\min} = 3.5$	$\theta_{\max} = 25.7$ , $\theta_{\min} = 2.8$	$\theta_{\max} = 25.7$ , $\theta_{\min} = 2.8$	$\theta_{\max} = 25.7$ , $\theta_{\min} = 3.0$
$(\sin \theta/\lambda)_{\max}$ (Å <sup>-1</sup> )	0.609	0.610	0.610	0.610
Range of $h, k, l$	$h = -15 \rightarrow 15, k = -14 \rightarrow 15, l = -15 \rightarrow 15$	$h = -18 \rightarrow 18, k = -19 \rightarrow 19, l = -11 \rightarrow 11$	$h = -10 \rightarrow 10, k = -11 \rightarrow 11, l = -16 \rightarrow 16$	$h = -11 \rightarrow 11, k = -14 \rightarrow 14, l = -15 \rightarrow 15$
$R[F^2 > 2\sigma(F^2)], wR(F^2), S$	0.026, 0.065, 1.16	0.033, 0.072, 1.18	0.039, 0.154, 1.11	0.036, 0.095, 1.02
No. of reflections	720	4162	3907	5461
No. of parameters	42	217	217	289
$\Delta\rho_{\max}, \Delta\rho_{\min}$ (e Å <sup>-3</sup> )	0.29, -0.71	1.16, -0.92	0.70, -1.58	1.26, -1.21

## Theoretical study of intermolecular noncovalent interactions I···I and Br···I in the crystal structure of 4

The full geometry optimization of cationic model structure  $[\text{SbIR}_3]^+$  and single point calculations for model tetrameric supramolecular associate  $\{[\text{SbIR}_3]^+\}_2 \cdots \{\text{I}_3^-\}_2$  based on the experimental X-ray geometry of **4** have been carried out at the DFT level of theory using the M06 functional [*Theor. Chem. Acc.* **2008**, *120*, 215.] with the help of the Gaussian-09 [Gaussian 09, Revision C.01, Gaussian, Inc., Wallingford, CT, **2010**.] program package. The Douglas–Kroll–Hess 2<sup>nd</sup> order scalar relativistic calculations requested relativistic core Hamiltonian were carried out using the DZP-DKH basis sets [*Mol. Phys.* **2010**, *108*, 1965. || *Chem. Phys. Lett.* **2013**, *582*, 158. || *J. Mol. Struct. - THEOCHEM* **2010**, *961*, 107. || *J. Chem. Phys.* **2009**, *130*, 064108.] for all atoms. No symmetry restrictions have been applied during the geometry optimization procedure. The Hessian matrix was calculated analytically for the optimized cationic model structure  $[\text{SbIR}_3]^+$  to prove the location of correct minima on the potential energy surface (no imaginary frequencies). The topological analysis of the electron density distribution with the help of the atoms in molecules (QTAIM) method developed by Bader and estimation of σ-hole values on the Sb, I, and Br atoms in the optimized equilibrium structure of  $[\text{SbIR}_3]^+$  have been performed by using the Multiwfn program (version 3.6) [*J. Comput. Chem.* **2012**, *33*, 580.]. The Chemcraft program [<http://www.chemcraftprog.com/>] was used for the visualization of electrostatic surface potential distribution and plotting of molecular orbitals. Results of interaction energy estimations for non-covalent interactions I···I and Br···I in model tetrameric supramolecular associate  $\{[\text{SbIR}_3]^+\}_2 \cdots \{\text{I}_3^-\}_2$  is shown in **Figures S1** and **S2**. The Cartesian atomic coordinates for all model structures are presented in **Table S5**.

**Table S4.** Values of the density of all electrons –  $\rho(\mathbf{r})$ , Laplacian of electron density –  $\nabla^2\rho(\mathbf{r})$  and appropriate  $\lambda_2$  eigenvalues (with promolecular approximation), energy density –  $H_b$ , potential energy density –  $V(\mathbf{r})$ , and Lagrangian kinetic energy –  $G(\mathbf{r})$  (a.u.) at the bond critical points, corresponding to intermolecular noncovalent interactions I···I and Br···I in model tetrameric supramolecular associate  $\{[\text{SbIR}_3]^+\}_2 \cdots \{\text{I}_3^-\}_2$ , bond lengths –  $l$  (Å), and estimated interaction energies –  $E_{\text{int}}$  (kcal/mol) for these contacts.<sup>‡</sup>

Contact*	$\rho(\mathbf{r})$	$\nabla^2\rho(\mathbf{r})$	$\lambda_2$	$H_b$	$V(\mathbf{r})$	$G(\mathbf{r})$	$l^{**}$	$E_{\text{int}}^a$	$E_{\text{int}}^b$
I100···I53 (Type II)	0.014	0.031	-0.014	0.001	-0.007	0.007	3.654	-3.0	-2.9
Br43···I53 (Type I)	0.009	0.027	-0.010	0.001	-0.005	0.006	3.692	-2.1	-2.5
Br43···I100 (Type I)	0.002	0.009	-0.003	0.001	-0.001	0.002	4.436	-0.4	-0.8

<sup>‡</sup> Results of QTAIM analysis did not reveal the presence of any appropriate bond critical points for intramolecular contacts Sb···O in model tetrameric supramolecular associate  $\{[\text{SbIR}_3]^+\}_2 \cdots \{\text{I}_3^-\}_2$  (the Poincare-Hopf relationship was satisfied during the QTAIM analysis and all critical points were determined).

\* Numeration of atoms in the model structure corresponds to their ordering in **Table S5**, Supporting Information. Two types of short halogen–halogen contacts are usually discussed in the literature [*Chem. Rev.* **2016**, *116*, 2478]. Type I is believed to depend on the effects of crystal packing, while type II is due to a classic halogen bonding (a halogen atom with a 90° angle provides its lone pair for interaction and the other one provides its  $\sigma$ -hole).

\*\* The shortest van der Waals radii for I and Br atoms are 1.98 and 1.83 Å, respectively. [*J. Phys. Chem.* **1966**, *70*, 3006.]

<sup>a</sup>  $E_{\text{int}} = 0.68(V(\mathbf{r}))$  (correlation developed for noncovalent interactions involving iodine atoms). [*Russ. Chem. Rev.* **2014**, *83*, 1181.]

<sup>b</sup>  $E_{\text{int}} = 0.67(-G(\mathbf{r}))$  (correlation developed for noncovalent interactions involving iodine atoms). [*Russ. Chem. Rev.* **2014**, *83*, 1181.]

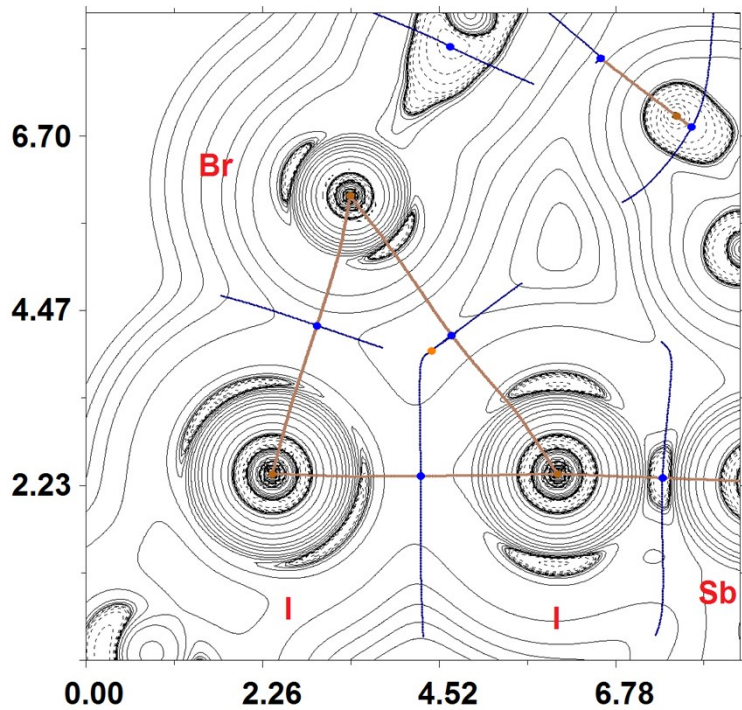


**Figure S1.** Contour line diagram of the Laplacian of electron density distribution  $\nabla^2\rho(\mathbf{r})$ , bond paths, and selected zero-flux surfaces referring to intermolecular noncovalent interactions I···I and Br···I in model tetrameric supramolecular associate  $\{[\text{SbIR}_3]^+\}_2 \cdots \{\text{I}_3^-\}_2$ . Bond critical points are shown in blue, nuclear critical points – in pale brown, ring critical points – in orange, length units – Å.

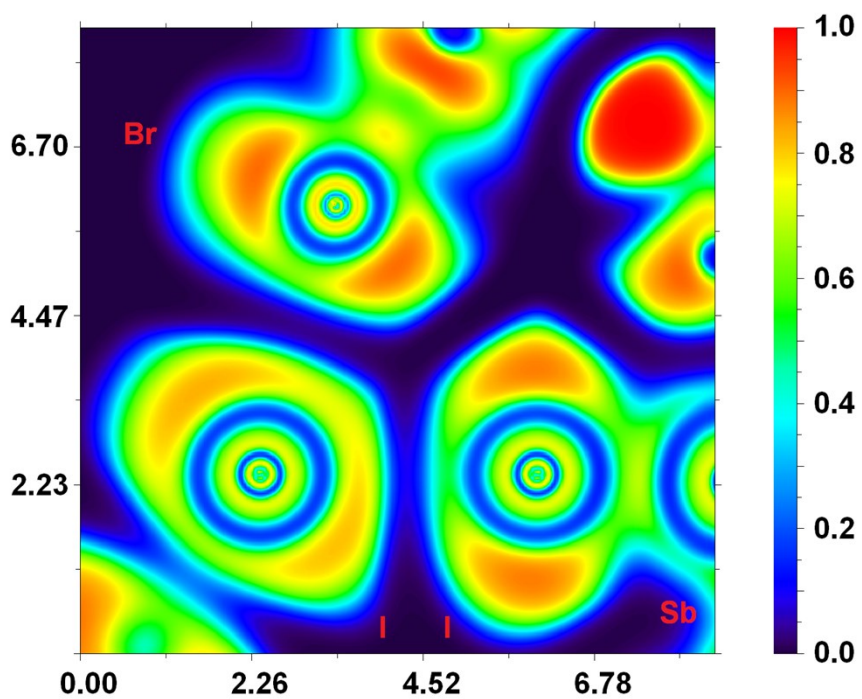


**Figure S2.** Visualization of electron localization function (ELF) for the intermolecular noncovalent interactions I...I and Br...I in model tetrameric supramolecular associate  $\{[\text{SbIR}_3]^+\}_2 \cdots \{\text{I}_3^-\}_2$ . The color scale for electron localization function is presented in a.u., length units – Å.

**Table S5.** Cartesian atomic coordinates for model structures.

Atom	X	Y	Z
Optimized equilibrium geometry of $[\text{SbIR}_3]^+$			
I	2.346528	-0.545498	-3.509547
Sb	4.036477	-2.590961	-3.162156
Br	2.256880	-3.559103	-8.700777
Br	8.677405	-2.219589	0.333328
Br	1.465043	-7.480147	-1.328075
O	5.549977	-4.796589	-3.819677

O	5.800582	-0.930876	-4.797145
O	3.643115	-1.958877	-0.312508
C	3.977212	-3.545820	-4.939080
C	4.872902	-4.622608	-4.983992
C	6.484199	-5.855618	-3.723061
H	7.289970	-5.743466	-4.472385
H	6.918628	-5.801063	-2.714086
H	5.987936	-6.835849	-3.853874
C	4.976885	-5.396264	-6.136973
H	5.658502	-6.249588	-6.198306
C	4.185947	-5.060143	-7.235095
H	4.257288	-5.659094	-8.149412
C	3.304492	-3.980102	-7.194886
C	3.196849	-3.212676	-6.036905
H	2.514842	-2.355604	-5.981062
C	5.878182	-1.916810	-2.709418
C	6.531098	-1.147182	-3.685549
C	7.828367	-0.690457	-3.446594
H	8.363951	-0.084420	-4.182120
C	8.451576	-1.015401	-2.246199
H	9.468831	-0.655801	-2.056449
C	7.806731	-1.788327	-1.281505
C	6.511629	-2.240462	-1.510416
H	6.001845	-2.847850	-0.753716
C	6.357943	-0.165776	-5.849250
H	6.585570	0.864239	-5.516562

H	7.275440	-0.639790	-6.246267
H	5.598840	-0.127518	-6.643846
C	3.227464	-3.745970	-1.723708
C	3.158250	-3.213484	-0.425818
C	2.620413	-3.981771	0.607622
H	2.567272	-3.602537	1.631877
C	2.124445	-5.249939	0.321292
H	1.695958	-5.852567	1.129370
C	2.158301	-5.766227	-0.973382
C	2.704998	-5.009096	-2.004010
H	2.730642	-5.411361	-3.023587
C	3.762526	-1.381003	0.975010
H	4.412721	-1.996985	1.626832
H	4.224686	-0.393171	0.832600
H	2.772491	-1.250789	1.450553
Tetrameric supramolecular associate $\{[\text{SbIR}_3]^+\}_2 \cdots \{\text{I}_3^-\}_2$			
C	3.151131	0.096817	5.732772
H	2.477713	0.543258	6.251810
H	3.883457	-0.150195	6.303714
H	2.776871	-0.693174	5.334411
C	2.867831	1.115943	3.617693
C	1.675979	0.561374	3.329627
H	1.282122	-0.023085	3.935604
C	1.047065	0.844086	2.166983
H	0.226890	0.445352	1.985319
C	1.577822	1.687922	1.267750

C	2.794157	2.255954	1.519483
H	3.188250	2.831737	0.904423
C	3.419813	1.953334	2.702889
C	2.960764	6.086926	3.874617
H	2.421691	6.049503	4.668745
H	2.396164	6.023755	3.101251
H	3.440600	6.918512	3.853855
C	5.405350	3.671034	4.977572
C	4.582636	4.779880	5.011310
C	4.531739	5.539677	6.159681
H	3.980089	6.286320	6.203799
C	5.295585	5.186916	7.226303
H	5.262255	5.694604	8.004860
C	6.114818	4.088063	7.161424
C	6.177183	3.309632	6.036409
H	6.727444	2.560722	5.997481
C	5.652827	1.402663	-0.986172
H	5.310395	2.023325	-1.633671
H	5.104369	0.615282	-0.978386
H	6.553652	1.162721	-1.218441
C	6.177798	3.207026	0.445075
C	6.081315	3.755144	1.692063
C	6.632188	4.958920	1.984022
H	6.575359	5.314612	2.841732
C	7.261513	5.621133	1.004338
C	7.349471	5.096001	-0.238757
H	7.793165	5.572898	-0.903126
C	6.807200	3.889570	-0.539799

H	6.865543	3.541033	-1.400104
O	3.608204	0.949979	4.733624
O	5.641014	1.994699	0.281578
O	3.880838	5.012823	3.878510
Br	0.720141	2.053285	-0.349831
Br	8.097391	7.231209	1.410745
Br	7.156847	3.634519	8.653917
Sb	5.311135	2.608709	3.190655
I	6.804919	0.450950	3.476126
I	11.635522	-3.568501	8.989085
I	10.247262	-3.024346	6.563622
I	8.854288	-2.526693	4.009048
I	-2.203322	3.568501	-8.989085
I	-0.815062	3.024346	-6.563622
I	0.577912	2.526693	-4.009048
C	6.281069	-0.096817	-5.732772
H	6.954487	-0.543258	-6.251810
H	5.548743	0.150195	-6.303714
H	6.655329	0.693174	-5.334411
C	6.564369	-1.115943	-3.617693
C	7.756221	-0.561374	-3.329627
H	8.150078	0.023085	-3.935604
C	8.385135	-0.844086	-2.166983
H	9.205310	-0.445352	-1.985319
C	7.854378	-1.687922	-1.267750
C	6.638043	-2.255954	-1.519483
H	6.243950	-2.831737	-0.904423
C	6.012387	-1.953334	-2.702889

C	6.471436	-6.086926	-3.874617
H	7.010509	-6.049503	-4.668745
H	7.036036	-6.023755	-3.101251
H	5.991600	-6.918512	-3.853855
C	4.026850	-3.671034	-4.977572
C	4.849564	-4.779880	-5.011310
C	4.900461	-5.539677	-6.159681
H	5.452111	-6.286320	-6.203799
C	4.136615	-5.186916	-7.226303
H	4.169945	-5.694604	-8.004860
C	3.317382	-4.088063	-7.161424
C	3.255017	-3.309632	-6.036409
H	2.704756	-2.560722	-5.997481
C	3.779373	-1.402663	0.986172
H	4.121805	-2.023325	1.633671
H	4.327831	-0.615282	0.978386
H	2.878548	-1.162721	1.218441
C	3.254402	-3.207026	-0.445075
C	3.350885	-3.755144	-1.692063
C	2.800012	-4.958920	-1.984022
H	2.856841	-5.314612	-2.841732
C	2.170687	-5.621133	-1.004338
C	2.082729	-5.096001	0.238757
H	1.639035	-5.572898	0.903126
C	2.625000	-3.889570	0.539799
H	2.566657	-3.541033	1.400104
O	5.823996	-0.949979	-4.733624
O	3.791186	-1.994699	-0.281578

O	5.551362	-5.012823	-3.878510
Br	8.712059	-2.053285	0.349831
Br	1.334809	-7.231209	-1.410745
Br	2.275353	-3.634519	-8.653917
Sb	4.121065	-2.608709	-3.190655
I	2.627281	-0.450950	-3.476126

### Hirshfeld Surface Analysis

The Hirshfeld molecular surfaces, shape index surfaces, and curvedness index surfaces were generated by CrystalExplorer program (version 17.5) [CrystalExplorer17, University of Western Australia, **2017**. <http://hirshfeldsurface.net>; *CrystEngComm* **2009**, *11*, 19.]. The normalized contact distances,  $d_{\text{norm}}$ , [*Chem. Commun.* **2007**, 3814.] based on Bondi's van der Waals radii, [*J. Phys. Chem.* **1966**, *70*, 3006.] were mapped into the Hirshfeld surfaces.

The **Figure S3** depicts the Hirshfeld surfaces for the cationic and anionic moieties in the crystal structure of **4** (mapping of the normalized contact distance  $d_{\text{norm}}$  was used for the visualization). In these Hirshfeld surfaces, the regions of shortest intermolecular contacts visualized by red circle areas. The main partial contributions of different intermolecular contacts to the Hirshfeld surfaces are given in **Table S6**. It is clear that despite the presence of multifold halogen···halogen contacts, the crystal packing determined primarily by intermolecular contacts involving hydrogen atoms as their fraction is maximal.

**Table S6.** Main partial contributions of different intermolecular contacts to the Hirshfeld surfaces for the cationic and anionic moieties in the crystal structure of **4**.

Moiety in <b>4</b>	Contributions of different intermolecular contacts to the molecular Hirshfeld surface*
Cationic	H–H 25.6%, Br–H 25.2%, I–H 18.3%, C–H 8.0%, I–C 6.5%, I–Br 3.9%, Br–C 3.2%, Br–Br 3.1%, C–C 2.4%, I–I 1.7%, O–H 1.2%
Anionic	I–H 61. 9%, I–C 20.1%, I–Br 9.6%, I–I 5.1%, I–O 2.6%

\* Contributions of other intermolecular contacts do not exceed 1%.

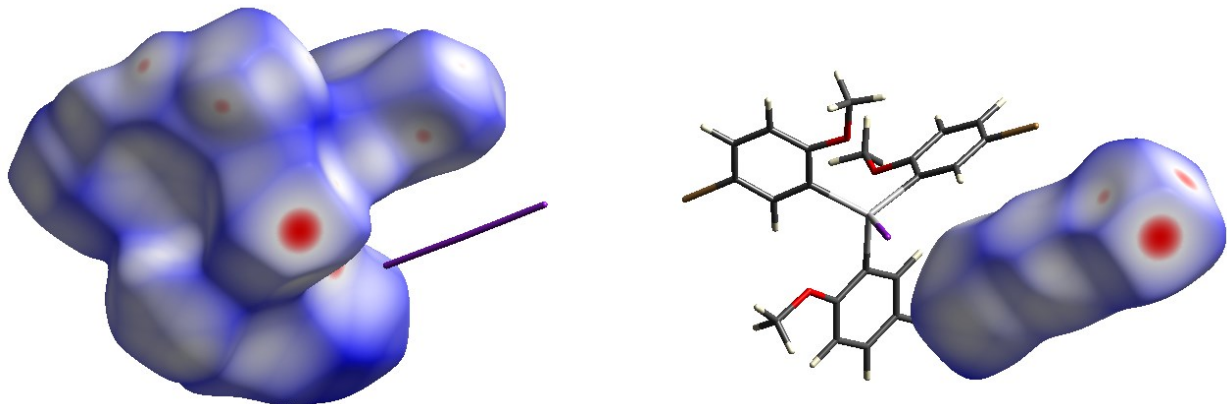


**Fig. S3.** Hirshfeld surfaces for cationic and anionic moieties in the crystal structure of **4**.

The parameters of morphology proper mean particles shape and appropriate surfaces provide basis for the optimal habit for the crystal. These parameters are useful for understanding of rheological attributes of the crystalline materials. The shape index (S) and curvedness (C) topological techniques [*CrystEngComm* **2009**, *11*, 19.] were employed for Hirshfeld surfaces of cationic and anionic moieties in the crystal structure of **5**. The technique S provides the local shape of the 3D surface and defines local topography (hollows and bumps in the 3D surface). The technique C represents the total curvature on the 3D surface and its mapping consists of flat green region separated by dark blue edges. The **Figure S4** shows the shape index surfaces and curvedness index surfaces plotted over the Hirshfeld surfaces of cationic and anionic moieties in the crystal structure of **4**.

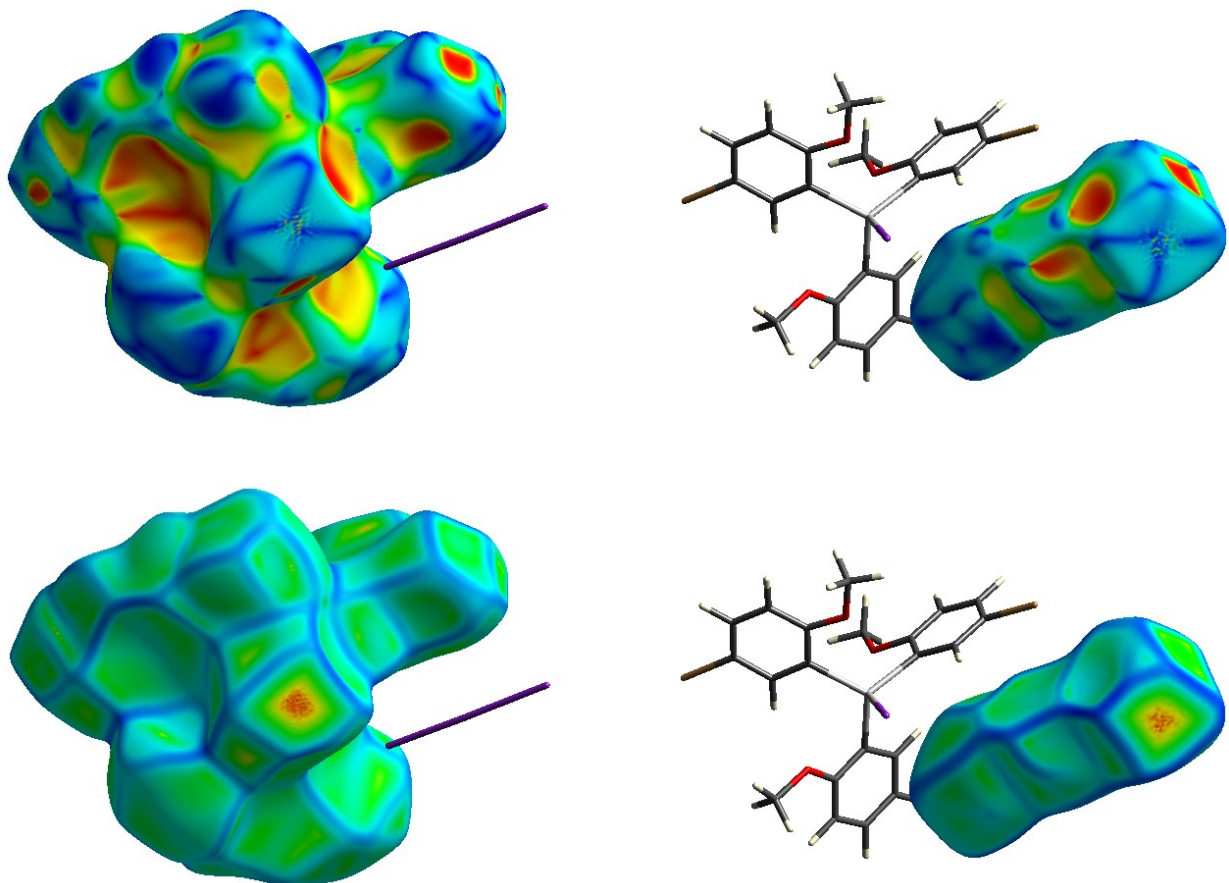


**Figure S4.** Shape index surfaces (top, color code: hollow – red; bumps – blue) and curvedness index surfaces (bottom, color code: edges – blue; flat regions – green) plotted over the Hirshfeld surfaces of cationic and anionic moieties in the crystal structure of **4**.

**Theoretical comparison of the thermodynamic favorability for the hypothetical reactions  $\text{Ar}_3\text{Sb} + 2\text{I}_2 \rightarrow [\text{Ar}_3\text{SbI}]^+ + \text{I}_3^-$  and  $\text{Ar}_3\text{Sb} + 2\text{I}_2 \rightarrow \text{Ar}_3\text{SbI}_2 + \text{I}_2$**

We carried out additional quantum chemical calculations at the PM7 [*J. Mol. Mod.* **2013**, *32*, 19.] level of theory with the help of MOPAC2016 program (Version: 20.160W) [J. J. P. Stewart, Stewart Computational Chemistry, web: <HTTP://OpenMOPAC.net>] in order to compare the thermodynamic favorability for the hypothetical reactions  $\text{Ar}_3\text{Sb} + 2\text{I}_2 \rightarrow [\text{Ar}_3\text{SbI}]^+ + \text{I}_3^-$  and  $\text{Ar}_3\text{Sb} + 2\text{I}_2 \rightarrow \text{Ar}_3\text{SbI}_2 + \text{I}_2$  (results are presented in **Tables S7** and **S8**). No symmetry restrictions have been applied during the geometry optimization procedure of all model structures. The Hessian matrices were calculated for all optimized model structures to prove the location of correct minima (reactants and products) on the potential energy surface (no imaginary frequencies in all cases). The Cartesian atomic coordinates for all optimized equilibrium model structures are presented in **Table S9**.

We found that both types of reactions are endothermic and close to equilibrium, the pathway  $\text{Ar}_3\text{Sb} + 2\text{I}_2 \rightarrow \text{Ar}_3\text{SbI}_2 + \text{I}_2$  is slightly more thermodynamically favorable than  $\text{Ar}_3\text{Sb} + 2\text{I}_2 \rightarrow [\text{Ar}_3\text{SbI}]^+ + \text{I}_3^-$  (only by 0.05 kcal/mol in terms of enthalpies).

**Table S7.** Calculated enthalpies (H, in cal/mol) of optimized equilibrium model structures at 298 K.

Optimized equilibrium model structure	H
Ar <sub>3</sub> Sb	19543.6411
I <sub>2</sub>	2404.6591
[Ar <sub>3</sub> SbI] <sup>+</sup>	20996.7646
I <sub>3</sub> <sup>-</sup>	3819.0765
Ar <sub>3</sub> SbI <sub>2</sub>	22364.6657

**Table S8.** Calculated enthalpies of hypothetical reactions Ar<sub>3</sub>Sb + 2I<sub>2</sub> → [Ar<sub>3</sub>SbI]<sup>+</sup> + I<sub>3</sub><sup>-</sup> and Ar<sub>3</sub>Sb + 2I<sub>2</sub> → Ar<sub>3</sub>SbI<sub>2</sub> + I<sub>2</sub> ( $\Delta H$ , in cal/mol).

Hypothetical reaction	$\Delta H$
Ar <sub>3</sub> Sb + 2I <sub>2</sub> → [Ar <sub>3</sub> SbI] <sup>+</sup> + I <sub>3</sub> <sup>-</sup>	462.9
Ar <sub>3</sub> Sb + 2I <sub>2</sub> → Ar <sub>3</sub> SbI <sub>2</sub> + I <sub>2</sub>	416.4

**Table S9.** Cartesian atomic coordinates for all optimized equilibrium model structures.

Atom	X	Y	Z
Ar <sub>3</sub> Sb			
C	6.4077	-0.5918	-6.2049
H	6.8472	-1.5743	-6.4001
H	5.6260	-0.3727	-6.9466
H	7.1663	0.1966	-6.2026
C	6.2844	-1.0996	-3.8822
C	7.6757	-1.0879	-3.7407
H	8.3147	-0.7139	-4.5339
C	8.2448	-1.5509	-2.5585
H	9.3289	-1.5454	-2.4396
C	7.4041	-2.0068	-1.5565
C	6.0159	-2.0305	-1.6941

H	5.4354	-2.4137	-0.8419
C	5.4192	-1.5960	-2.8794
C	6.1391	-5.5216	-3.2265
H	7.0454	-5.1664	-3.7250
H	6.2588	-5.4685	-2.1335
H	5.8734	-6.5385	-3.5315
C	3.7772	-3.2674	-4.8533
C	4.6930	-4.3398	-4.7160
C	5.1615	-5.0698	-5.8137
H	5.8734	-5.8795	-5.6873
C	4.6964	-4.7571	-7.0869
H	5.0591	-5.3198	-7.9486
C	3.7700	-3.7361	-7.2252
C	3.2993	-2.9976	-6.1374
H	2.5542	-2.2137	-6.3428
C	3.7233	-1.6229	1.3845
H	4.6161	-2.1935	1.6599
H	3.9542	-0.5483	1.3418
H	2.8957	-1.8094	2.0753
C	3.1030	-3.1835	-0.3157
C	2.9796	-3.4031	-1.7071
C	2.6708	-4.7051	-2.1130
H	2.5189	-4.9829	-3.1694
C	2.5557	-5.7265	-1.1680
C	2.7162	-5.5049	0.1896
H	2.6342	-6.3148	0.9157
C	2.9869	-4.2107	0.6252
H	3.0997	-4.0198	1.6871

O	5.6772	-0.5734	-4.9863
O	3.3283	-1.8884	0.0477
O	5.0505	-4.6342	-3.4392
Br	8.1614	-2.6512	0.0626
Br	2.1877	-7.4887	-1.7730
Br	3.1276	-3.3154	-8.9636
Sb	3.2777	-1.8709	-3.2430
I <sub>2</sub>			
I	0.186042	0.000000	0.000000
I	-0.186042	0.000000	0.000000
[Ar <sub>3</sub> SbI] <sup>+</sup>			
C	6.6510	0.1021	-5.8636
H	7.5943	-0.3391	-6.2022
H	5.9161	0.1147	-6.6843
H	6.7898	1.1084	-5.4529
C	6.6159	-0.9996	-3.7353
C	7.9084	-0.5505	-3.4291
H	8.4772	0.0462	-4.1416
C	8.4670	-0.8750	-2.2033
H	9.4793	-0.5317	-1.9562
C	7.7265	-1.6381	-1.2996
C	6.4453	-2.0860	-1.5885
H	5.9333	-2.6838	-0.8122
C	5.8480	-1.7711	-2.8278
C	6.4144	-6.1385	-3.9198
H	7.2286	-5.9058	-4.6142
H	6.7717	-6.1097	-2.8781
H	5.9465	-7.1048	-4.1392

C	3.9333	-3.6716	-4.9841
C	4.7809	-4.8058	-5.0648
C	4.8982	-5.5772	-6.2286
H	5.5709	-6.4330	-6.2691
C	4.1403	-5.2428	-7.3396
H	4.2201	-5.8418	-8.2551
C	3.2793	-4.1466	-7.2695
C	3.1681	-3.3650	-6.1276
H	2.4622	-2.5187	-6.1692
C	3.7266	-1.4444	1.2378
H	4.3295	-2.0655	1.9091
H	4.2115	-0.4688	1.0725
H	2.7051	-1.3073	1.6084
C	3.1732	-3.2050	-0.2953
C	3.1865	-3.6271	-1.6472
C	2.6684	-4.9125	-1.9215
H	2.6407	-5.3419	-2.9399
C	2.1685	-5.6968	-0.8919
C	2.1463	-5.2552	0.4322
H	1.7370	-5.8860	1.2311
C	2.6521	-4.0005	0.7341
H	2.6393	-3.6471	1.7644
O	6.0061	-0.7425	-4.9161
O	3.7188	-1.9843	-0.0795
O	5.4409	-5.0996	-3.9181
Br	8.4912	-2.0721	0.3738
Br	1.4946	-7.4161	-1.2905
Br	2.2356	-3.7142	-8.7842

Sb	3.9282	-2.4916	-3.2455
I	2.2961	-0.4181	-3.6522
$I_3^-$			
I	11.7332	-3.6216	9.1228
I	10.3827	-3.0387	6.8972
I	8.6211	-2.4592	3.5418
$\text{Ar}_3\text{SbI}_2$			
C	-0.2771	1.1654	4.4312
C	-1.9562	0.3945	2.9236
C	-2.8602	0.0914	3.9485
C	-4.0121	-0.6219	3.6454
C	-4.2382	-0.9998	2.3269
C	-3.3428	-0.7103	1.3011
C	-2.1478	-0.0335	1.5916
C	3.6575	0.1890	-1.3877
C	0.8563	1.6673	0.3542
C	2.1556	1.6107	-0.1955
C	3.1685	2.5036	0.1759
C	2.8795	3.5171	1.0799
C	1.5862	3.6214	1.5793
C	0.5764	2.7295	1.2297
C	-2.7268	-3.8904	-0.5605
C	-1.3233	-2.3483	-1.7307
C	-0.6179	-1.1271	-1.6397
C	0.2248	-0.7911	-2.7106
C	0.3889	-1.6822	-3.7679
C	-0.2730	-2.9025	-3.8237
C	-1.1463	-3.2381	-2.7972

O	-0.8728	1.1912	3.1398
O	-2.2235	-2.5731	-0.7374
O	2.3402	0.6768	-1.1674
Br	-5.8260	-1.9528	1.9137
Br	1.5660	-1.2172	-5.1810
Br	1.1856	5.0296	2.7857
Sb	-0.6584	0.1778	0.0632
I	0.9425	-1.6924	1.4423
I	-2.2561	1.9865	-1.3259
H	-0.1186	0.1397	4.7780
H	0.6892	1.6585	4.2456
H	-0.8795	1.7482	5.1340
H	-2.6739	0.4180	4.9674
H	-4.7231	-0.8674	4.4368
H	-3.6203	-1.0303	0.2805
H	4.1144	-0.1525	-0.4538
H	3.4732	-0.6649	-2.0576
H	4.2661	0.9471	-1.8889
H	4.1667	2.4191	-0.2435
H	3.6607	4.2193	1.3785
H	-0.4247	2.9055	1.6664
H	-1.9133	-4.6124	-0.4414
H	-3.2912	-3.7913	0.3793
H	-3.3958	-4.1583	-1.3838
H	0.7774	0.1650	-2.7678
H	-0.1243	-3.5927	-4.6570
H	-1.6852	-4.1798	-2.8364

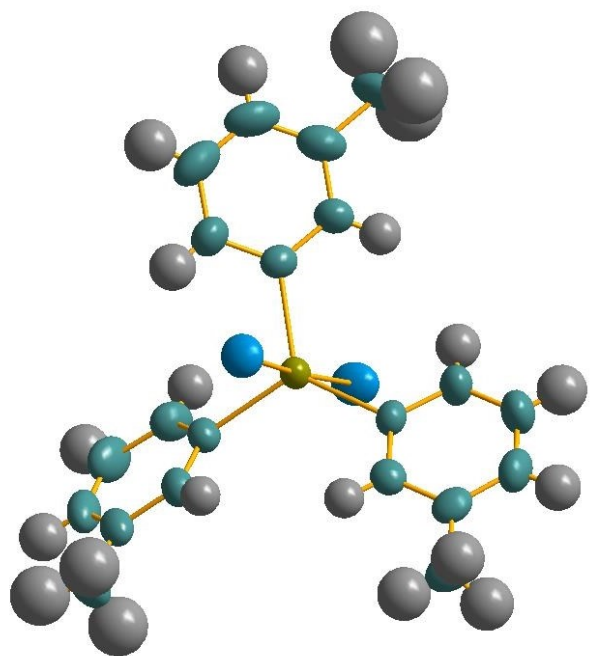


**Figure S5.** Structure of **2** given in thermal ellipsoids